Front. Chem. Sci. Eng.
https://doi.org/10.1007/s11705-018-1722-y

REVIEW ARTICLE

Recent advances on metal-free graphene-based catalysts for the production of industrial chemicals

Zhiyong Wang[1,2], Yuan Pu[1,2], Dan Wang (✉)[1,2], Jie-Xin Wang[1,2], Jian-Feng Chen[1,2]

1 Beijing Advanced Innovation Center for Soft Matter Science and Engineering, State Key Laboratory of Organic-Inorganic Composites, Beijing University of Chemical Technology, Beijing 100029, China
2 Research Center of the Ministry of Education for High Gravity Engineering and Technology, Beijing University of Chemical Technology, Beijing 100029, China

Abstract With the development of carbon catalysts, graphene-based metal-free catalysts have drawn increasing attention in both scientific research and in industrial chemical production processes. In recent years, the catalytic activities of metal-free catalysts have significantly improved and they have become promising alternatives to traditional metal-based catalysts. The use of metal-free catalysts greatly improves the sustainability of chemical processes. In view of this, the recent progress in the preparation of graphene-based metal-free catalysts along with their applications in catalytic oxidation, reduction and coupling reactions are summarized in this review. The future trends and challenges for the design of graphene-based materials for industrial organic catalytic reactions with good stabilities and high catalytic performance are also discussed.

Keywords graphene-based materials, metal-free catalyst, industrial chemical productions, catalytic reaction

1 Introduction

In the production of industrial chemicals, more than 85% of the reactions need to be carried out with a catalyst [1]. Organic synthesis reactions such as the dehydrogenation of hydrocarbons, the reduction of aromatic nitro compounds and coupling reactions are all important catalytic reactions in industry [2]. In the past, these reactions were generally catalyzed by Al, Mn, Ni, or Cu since these catalysts are cheap and suitable for industrial mass production [3]. However, due to limited resources and environmental pollution, the large-scale use of metal based catalysts in industry is increasingly being subjected to more regulations and experiencing other challenges [4–7]. In recent decades, the carbon family has gained several new members such as activated carbon, graphite, graphite intercalation compounds, and carbon fibers [8–10]. With the development of green chemistry and sustainable chemistry, the application of these metal-free carbon-based materials as catalysts for the production of industrial chemicals is gradually being explored more and more [11–13].

Some graphene-based materials synthesized by chemical oxidation reduction methods have abundant oxygen-containing functional groups, including hydroxyl, carbonyl, carboxylic acids and epoxy groups [14–16]. These groups give the graphene-based catalyst excellent catalytic oxidation performance. In addition, the heteroatom doping of graphene can alter the electronic and spin structure of carbon materials, which endows them with better catalytic activities [17,18]. In fact, graphene-based metal-free nanomaterials have been applied to many types of metal-catalyzed processes, and they are expected to replace traditional metal-based catalysts [19,20]. This is significant because these substitutions save metal resources and improve the sustainability of chemical processes.

This short review presents the latest developments in the use of graphene-based catalysts in industrial organic reactions. First, a brief introduction of the fabrication and catalytic active sites of intrinsic graphene, graphene oxide (GO), reduced graphene oxide (rGO), heteroatom doped graphene, and macroscopic graphene-based frameworks is presented. Then recent progress in the design and fabrication of these graphene-based catalysts and their catalytic performance in organic reactions, including oxidation, reduction and other important industrial reactions are summarized. Finally, the future trends, opportunities, and challenges of graphene-based materials for industrial productions are discussed.

Received January 23, 2018; accepted March 3, 2018

E-mail: wangdan@mail.buct.edu.cn

2 Preparation of graphene-based materials for metal-free catalysts

2.1 Graphene

Graphene is a two-dimensional layered material obtained from a repeated arrangement of carbon atoms in a hexagonal unit [21]. Every carbon atom in the graphene sheet is bonded to three neighboring carbon atoms and is sp^2 hybridized with the remaining unhybridized p_z orbital oriented perpendicular to the graphene plane. Stacked rings undergo π-π interactions between the planes. The first high-quality graphene sheets were obtained via mechanical exfoliation by Novoselov et al. in 2004 [22]. The advent of graphene enriched the carbon family and graphene became the basic unit of other graphite materials [23]. Due to its unique structural and physicochemical properties, graphene has been widely applied to various fields such as catalysts, absorbents, sensors, biological applications, transparent conductive electrodes, and energy storage [24]. This review focuses on the applications of graphene to catalysis.

Although the hybrid orbital forms are similar between graphene and other graphite materials (like graphite, fullerene and carbon nanotubes), graphene possesses a huge and open π electronic system, which is beneficial for interactions between the graphene sheets and the reactant molecules [25–27]. In addition, the two special edge structures, armchair and zigzag, provide extra electronic states for graphene and produce new energy levels at the Fermi level, which greatly reduce the difficulty for catalytic reactions proceed [28].

Recently, a great deal of research has focused on preparing high-quality graphene sheets. In addition to the already mentioned mechanical exfoliation method, other commonly used methods include chemical vapor deposition, oxidation-reduction method, solvothermal and arc methods [29–32]. Each of these methods has advantages and drawbacks. Mechanical exfoliation gives high-quality graphene but with low yields, which is a problem for large-scale production. Chemical vapor deposition produces high-quality and high-volumes of graphene, but its high cost and complex process hinders its industrialization. Overall oxidation graphite reduction is the best method for the large-scale preparation of graphene due to its low cost and simplicity.

2.2 Graphene derivatives

2.2.1 Graphene oxide

It is difficult to fabricate graphene with an ideal two-dimensional structure. As mentioned above, reducing GO is the most commonly used method for the fabrication of high quality graphene. The structure of GO is controversial, but currently the structure proposed by Lerf et al. which is shown in Fig. 1 is the most widely acceptable [33]. Typically, GO contains a large number of oxygen-containing functional groups. Most of these groups exist in the graphene oxide layer in the form of hydroxyl and epoxy groups, although a small number of carboxyl and carbonyl groups exist on the lamellar edges of graphene oxide sheets. However, these oxygen-containing functional groups destroy the intrinsic extensive π electronic system that an ideal graphene system would possess [34].

Theoretically, the catalytic activity will be lower when the giant π-conjugated distribution is reduced [35]. However for most oxidation reactions, the radical oxygen species easily interact with the oxygen containing groups on the GO sheets, this together with the hydrophilicity and ready dispersibility in water caused by these groups, gives GO an excellent catalytic performance in oxidation reactions [36]. GO is usually prepared via modified Hummers' methods by using $KMnO_4$, H_2SO_4, or $NaNO_3$ as oxidants [37]. Chen et al. fabricated single-layer GO with a high yield of 171%±4% via a modified Hummers' method by using small flakes (3–20 μm) as the raw material. Dispersions of the obtained GO were high purity and did not require any follow-up procedures such as centrifugation or dialysis. This method provides an efficient way for the inexpensive and simple mass-production of graphene for industrial processes [38]. In addition to the universal Hummers' method, Bai et al. prepared GO with a controllable-oxygen-content by irradiating graphite with a high energy electron beam [39]. This beam produced varying degrees of damage in the graphite structure and the oxygen containing functional groups on the surface of GO, especially the hydroxyl and carboxyl groups, increased with increasing irradiation doses.

2.2.2 rGO

A GO reduction process can restore some of the intrinsic graphene properties [40]. As shown in Fig. 1, after GO is reduced, the π electronic structure is enlarged to some extent. The reduction process eliminates the hydroxyl and epoxy groups while retaining most of carboxyl and carbonyl groups at the edges of the GO sheet [41]. So the reduction is not complete. Chemical reduction, using reducing agents such as sodium borohydride, hydrazine hydrate, or hydroquinone, is an efficient and safe way for reducing GO [42,43]. Nevertheless, the rGO obtained by this method may not be pure due to the presence of the reducing agents. For example, when GO is reduced by hydrazine hydrate, nitrogen from the reducing agent is introduced into the rGO. In addition, as shown in Fig. 1(b), many defects are introduced into the rGO basal plane [44]. These defects result in a large mass loss (about 30%) and a change in the electronic arrangement of the electrons [45].

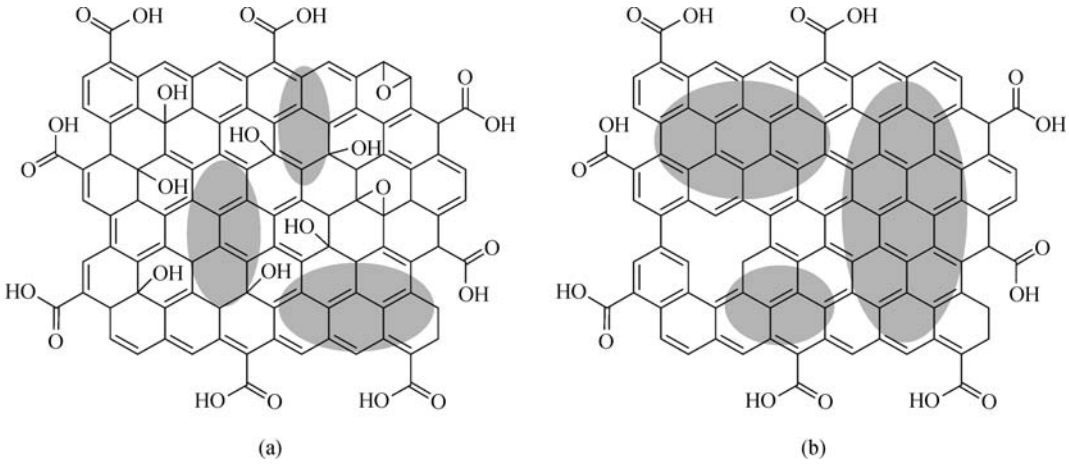

Fig. 1 Structure diagram of (a) GO and (b) rGO

2.2.3 Heteroatom-doped graphene

As mentioned above, the armchair and zigzag edge structures and the huge π electronic system are the main active sites in graphene. Whereas the main active sites in GO are the oxygen groups on the defects sites. The introduction of heteroatoms can also alter the electronic and spin structures of graphene and as shown in Fig. 2, these heteroatoms become active catalytic sites [46–48]. Generally, there are two main methods for the fabrication of heteroatom-doped graphene catalysts, the post-treatment of GO and *in situ* growth [49].

Fig. 2 Schematic diagram of active sites of graphene derivatives

N-doped graphene was first prepared via an *in situ* chemical vapor deposition (CVD) growth method which used CH_4 and NH_3 as the C and N sources, respectively [50]. Most of the N-doped graphene prepared by this method had structures with only a few layers and the layers contained some defects. Other heteroatoms such as Si, B, S, and P can also form covalent bonds with graphene. The chemical properties of these doped materials are very different from each other due to the different electronegativities of these heteroatoms [51–54]. Xu and coworkers reported a large-scale production of sulfurized edge-functional graphene using ball milling methods [55]. The as-prepared metal-free material exhibited excellent performance in lithium-sulfur batteries with an initial reversible capacity of 1265.3 $mAh \cdot g^{-1}$ at 0.1 C in the voltage range of 1.5–3.0 V. Other halogenated edge-functional graphene nanoplatelets (XGnPs, X = Cl, Br, or I) prepared by the same method have also been reported [56,57].

The co-doping of two or more heteroatoms has been found to further enhance the catalytic activity of graphene due to a synergic effect [58]. Zhang et al. developed a multifunctional tri-doped graphene electrocatalyst with nitrogen, phosphorus, and fluorine [59]. The catalyst was prepared by the thermal activation of a mixture of polyaniline, GO and ammonium hexafluorophosphate and was efficient for oxidation reduction reaction, oxygen evolution reaction, and hydrogen evolution reaction.

2.3 Macroscopic graphene-based frameworks

Macroscopic 3D structured graphene catalysts have higher specific surface areas than graphene planes so in recent years their applications as organic catalysts have increased rapidly [60]. Several methods have been reported for the manufacture of 3D monolith graphene-based materials and many of these methods require harsh conditions. For example, in the earlier years, graphene foam prepared from polyurethane foam usually required reaction temperatures up to 3000 °C [61]. However, with the optimization of the raw and processed materials, graphitization can now be conducted at temperatures as low as 900 °C [62]. Xia et al. fabricated three-dimensional porous graphene like sheets (3DPGLS) directly from biocarbons at 900 °C [63]. The as-obtained 3DPGLS had a high specific surface area (1506.19 $m^2 \cdot g^{-1}$) and a low defect density.

Structured graphene foams can also be prepared by CVD methods, which are performed at relatively low temperatures (400–800 °C) [64]. Materials obtained by this method generally retain many of the chemical properties of pristine graphene. By using a facile one-step plasma-enhanced chemical vapor deposition method, a hierarchical graphene foam was fabricated and then utilized as an efficient solar-thermal conversion medium (solar-vapor conversion efficiency ≈ 91.4%) [65]. The hydrothermal and freeze-drying treatment of graphene oxide is an even simpler method which yields macroscopic columnar rGO aerogels [66].

Another hot research area is 3D printing technology since it can print specific three-dimensional structured materials [67]. Recently, it has been applied to the preparation of three-dimensional graphene macro bodies at the centimeter level. In 2015, Zhu et al. were the first to used 3D printing to fabricate graphene aerogels with periodic arrays [68]. The 3D printed graphene aerogels were ultralightweight, highly conductive and super compressible (up to 90% compressive strain). Sha and coworkers used a layer-by-layer self-assembly method to fabricate a multi-layer graphene foam from Ni and a solid carbon source [69]. A carbon dioxide laser was used as the heat source. The Ni was simultaneously used as the template and catalyst for graphene growth and the 3D printed graphene foam had high porosity (~99.3%), low density (~0.015 $g \cdot cm^{-3}$), high-quality and multilayered graphene features.

3 Graphene-based materials in catalytic reactions

3.1 Oxidation reactions

Many industrial chemicals and intermediates are organic compounds such as acids, aldehydes and ketones all of which contain oxygen and all of which can be obtained by oxidation [70]. Oxidation reactions account for the highest proportion (more than 30%) of chemical reactions used in the production of organic chemicals [71]. Phenol is one of the most important intermediates in industrial synthesis reactions [72]. It is most commonly produced by a three-step cumene process which has many problems such as high-energy consumption, metal solid waste pollution, and low yield [73]. To address these problems, a chemically converted graphene (CCG) prepared by the exfoliation of graphite has been used as a metal-free catalyst for the oxidation of benzene to phenol in the presence of hydrogen peroxide (Scheme 1) [74]. The conversion of benzene was 18% and no byproducts were formed. The outstanding catalytic performance is believed to be related to the decomposition rate of H_2O_2, the adsorption ability of the reactant, and a balanced kinetic control process. The CCG could be reused seven times with no obvious decrease in the catalytic performance.

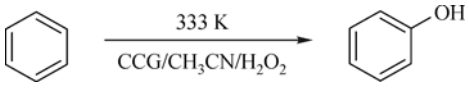

Scheme 1 Oxidation of benzene using CCG as catalyst [74]

In industrial processed, phenol is often further oxidized to other useful products. Indrawirawa and co-workers fabricated nitrogen-doped reduced graphene oxide (N-rGO) at low temperatures using ammonium nitrate as the N source [75]. The N-rGO was then used directly as a metal-free catalyst for the oxidation of phenol and it had a significantly better catalytic activity for the degradation of phenol than rGO (90% *versus* 50% within 2 h). The catalytic activity of N-rGO was related to the annealing temperature and it can be improved as the temperature increasing. In addition, the effect of the reaction temperature on the phenol oxidation rate constant was investigated and this catalytic system was shown to follow a first-order reaction when activated by peroxymonosulfate (PMS). The activation energy was calculated to be 31.6 $kJ \cdot mol^{-1}$.

Besides monatomic doped graphene, a sulfur and nitrogen co-doped graphene (SNG) was also applied to the same reaction system [76]. The PMS activation process was studied using electron paramagnetic resonance (EPR) in order to obtain the catalytic reaction mechanism. As shown in Fig. 3(a), SNG efficiently activates PMS to generate active radicals. The number of $SO_4^{\bullet-}$ and $^{\bullet}OH$ active radicals in the mixture both increased during the first five minutes and then decrease as the phenol was consumed by the oxidation process (Fig. 3(b)). This radical generation process with PMS is much different from that the processes catalyzed by metal-based material, which only actives PMS generating $^{\bullet}OH$ initially in the first few minutes and the concentration of $SO_4^{\bullet-}$ climbed up afterwards [77].

The selective oxidative dehydrogenation of ethylbenzene to styrene is another widely used industrial chemical process for the synthesis of resins, rubbers, and dyes (Scheme 2) [78]. A metal-free rPGO catalyst with a high specific surface area (2613 $m^2 \cdot g^{-1}$) was prepared by a microwave assisted exfoliation method and then used in the catalytic oxidative dehydrogenation of ethylbenzene (EB) to styrene (ST). The conversion of EB and the selectivity of ST were 65% and 93%, respectively. When rPGO was compared to other carbon catalysts (oxidized carbon nanotubes, rGO, and graphite powder), it showed the best catalytic performance for the oxidative dehydrogenation of EB reaction (Fig. 4). This is due to its high porosity and novel pore structure. These features enhance the mass and heat transfer during the reaction and lead to a high ST selectivity.

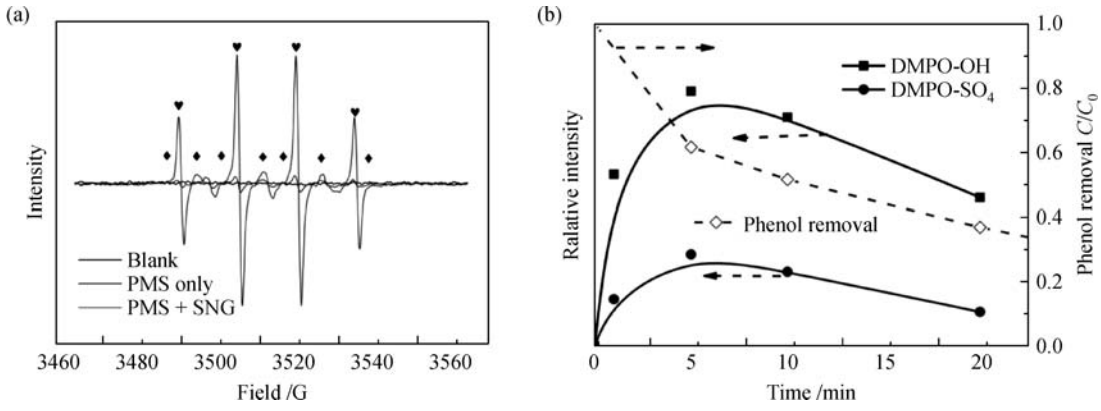

Fig. 3 (a) EPR spectra of PMS activation under different conditions (♥: DMPO-OH, ♦: DMPO-SO_4); (b) radical evolution during the PMS activation on SNG (catalyst: 0.2 $g \cdot L^{-1}$; PMS: 6.5 × 10^{-3} $mol \cdot L^{-1}$; phenol: 20 $mg \cdot L^{-1}$; T: 25 °C; DMPO: 0.08 $mol \cdot L^{-1}$) [76]

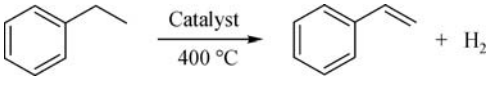

Scheme 2 Selective oxidative dehydrogenation of ethylbenzene to the styrene [78]

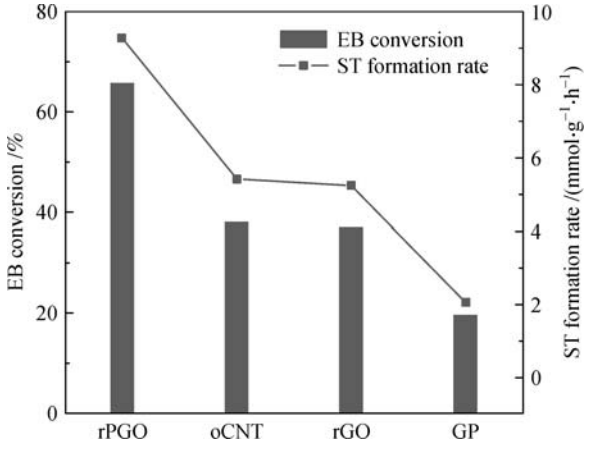

Fig. 4 Catalytic performance of different carbon materials during the oxidative dehydrogenation of EB, after 30 h on stream. Reaction conditions: 50 mg of the catalyst, 3% EB with He balance, O_2-EB = 1, total flow rate = 10 $mL \cdot min^{-1}$, T = 400 °C [78]

ST can be further oxidized to the corresponding benzaldehyde by using sulfur doped graphene (SG) as the catalyst. However, in contrast, rGO exhibits negligible activity under the same reaction conditions [79]. Other 3D-structured carbon catalysts with higher specific surface areas than CNTs and graphene planes have also been developed for use as organic reaction catalysts. Gonçalves and co-workers found that a three-dimensional graphene oxide foam (3DGO) was more efficient than two-dimensional graphene oxide sheet (2DGO) when used as a metal-free catalyst for the oxidation of thioanisole (3DGO: conversion 87% and S = O selectivity 91.2% *versus* 2DGO: conversion 65% and S = O selectivity 60.5%) [80]. A representative group of graphene-based materials that have been used for oxidation catalytic reactions are summarized in Table 1.

3.2 Reduction reactions

The hydrogenation reductions of nitro compounds to corresponding aromatic amines are important organic reactions both in industrial applications and in academic research. The reaction products are intermediates for many chemicals such as pharmaceuticals, dyes, and plastics. The reduction process of nitroarenes by borohydride in aqueous solution can be measured directly by UV-vis spectroscopy, and the reaction only takes several minutes [84]. Therefore, this reaction is often used for the determination of catalyst activity and kinetic studies.

The reaction mechanism for the reduction of nitroarene catalyzed by carbon-based materials has been extensively studied. By using an *in situ* infrared characterization technique, Kong and coworkers showed that 4-nitrophenol (4-NP) ions tended to interact with NG via the O atom of the hydroxyl group [46]. The rate determining step of the reaction is the adsorption of the 4-nitrophenol ions giving the reaction pseudo-zero-order kinetics. This is completely different from the pseudo-first-order reactions catalyzed by metal nanoparticles.

Wang and coworkers studied the reaction mechanism for the reduction of 4-NP catalyzed by edge SG [85]. The reductant was first adsorbed on the surface of the catalyst because the adsorption capacity of SG for $NaBH_4$ is greater than that of 4-NP (as determined by the first principle based on the density functional theory). The adsorbed $NaBH_4$ was then transformed into active hydrogen species which reacted with the adsorbed 4-NP molecules to generate the products on the surface of SG (Scheme 3).

A three-dimensional nitrogen-doped graphene foam

Table 1 Graphene-based materials used in oxidation catalytic reactions

Catalyst	Reaction system	Reaction conditions				Level		Ref.
		Cat. dosage /mg	Capacity /mmol	Temp. /K	Time /h	Conv. /%	Select. /%	
Graphene	Benzyl alcohol oxidation to benzaldehyde	30	0.1	313	10	0.4	100	[81]
N-doped graphene (NG)		30	0.1	313	10	3.5	100	
		30	0.1	343	10	3.5	100	
CCG	Oxidation of benzene to phenol	20	1.67	333	8	18	97	[74]
2DGO	Oxidation of thioanisole to sulfoxide	4	0.3	298	24	65	60.5	[80]
3DGO		4	0.3	298	24	87	91.2	
Porous rGO	Oxidativedehydrogenation of ethylbenzene to styrene	50	0.025	673	30	65	97	[78]
SG	Oxidation of styrene to benzaldehyde	10	8.7	373	7	13	70	[79]
GO	Oxidation of 5-Hydroxymethylfurfural into 2,5-diformylfuran	50	1	373	12	67.4	98.4	[14]
NG	Glucose oxidation to succinic acid	25	0.5	433	20	100	68	[82]
rGO	Oxidative thiophene desulfurization	5	0.32	413	6	100	–	[83]

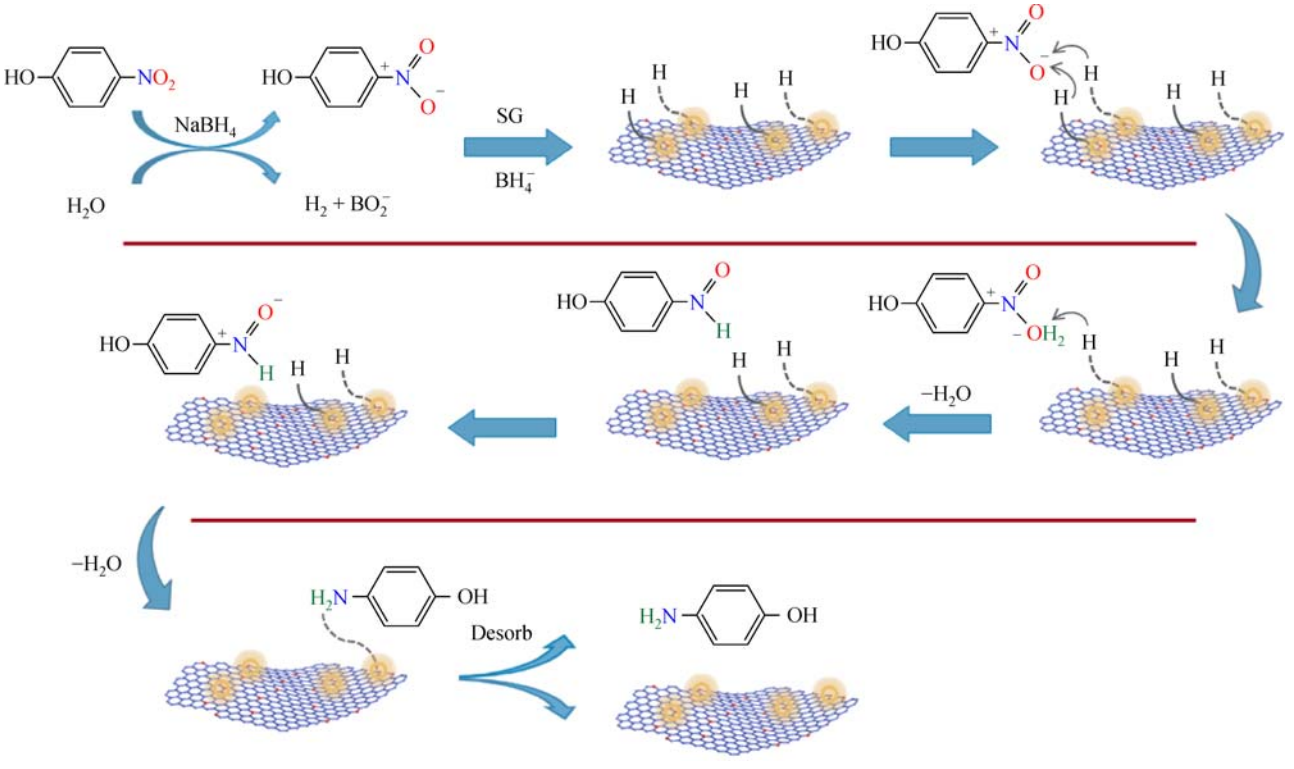

Scheme 3 The reaction mechanism for the reduction of 4-NP to 4-AP catalyzed by SG metal-free catalyst [85]

(3D-NGF) was prepared via a one-step hydrothermal method and used as the reduction catalyst in the same reaction system [86]. The 4-NP was completely converted within 18 min at room temperature. The specific rate constant and apparent rate constant of 3D-NGF were calculated to be 4.94×10^{-4} mol·L^{-1}·s^{-1}·g^{-1} and 0.2391 min^{-1}, respectively. The 3D-NGF catalyst was easily separated for reuse an exhibited excellent durability with a decrease of only 4% in catalytic activity after seven cycles. A S-N-codoped hollow carbon nanosphere/graphene aerogel (SNC-GA-1000), which was fabricated using a facile and clean solid ion transition route, completely converted 4-NP to 4-AP within 7 min after five cycles [87]. These results show that the catalytic activity of multi-heteroatom doped carbon-based materials is higher than that of single heteroatom doped catalysts.

Catalysts fabricated by self-assembly methods without hard templates often have fluffy carbon framework structures so they cannot meet the high strength and mass transfer requirements of traditional industrial reactors [88]. So, Wang and coworkers used nickel foam as a skeleton and via a hydrothermal method fabricated 3D structured nitrogen doped graphene coated nickel foam (NG/NF) [89]. The NG/NF is an efficient catalyst for the reduction of nitrobenzene to aniline which can be attributed to the strong van der Waals adhesions of GO to the surface of the nickel metal. The mass loss of NG/NF was below 1 wt-% throughout sonication treatment (up to 30 min), which illustrates the excellent stability of NG/NF. The kinetics of the catalytic process was studied under various conditions and the data fit well to a Langmuir-Hinshelwood model with an error ratio below 10%. Representative graphene-based materials that have been used in catalytic reduction reactions are summarized in Table 2.

3.3 Coupling reactions

In addition to oxidation and reduction reaction, there are some other important industrial reactions that have been catalyzed by graphene catalysts. For example, Friedel-Crafts alkylation reactions can be directly catalyzed by graphene oxide (Scheme 4) [92]. This reaction has a high conversion of arenes and excellent regioselectivity of the corresponding products. It is believed that both coupling partners are probably activated because of the abundant polar oxygen groups and holes in the graphene layers. Gao et al. also reported graphene oxide as a metal-free catalyst for the direct alkylation reaction of iodobenzene and benzene [93]. There was a linear correlation between the yield of the target products and the oxygen content of graphene oxide.

Another important addition reaction, the Michael addition (Scheme 5), can be catalyzed by diethylenetriamine modified graphene oxide (GO-DETA) [94]. The catalytic activity was evaluated using (E)-chalcone and malononitrile and the (E)-chalcone was entirely transformed to the corresponding product within 2 h.

Li and Antonietti developed a boron and nitrogen codoped holey graphene monolith (BNHG) via the copolymerization of glucose and boric acid [95]. The BNHG exhibited an efficient conversion (91%) and excellent selectivity ($>99\%$) for the oxidative coupling of amine into imine (Scheme 6). Theoretical calculations were used to show that the high catalytic activity of BNHG was due to the introduction of boron and nitrogen atoms, which induced electron rearrangements in both the conduction and valence bands.

Yang et al. found that a phosphorus-doped nanomesh graphene (PG) catalyzed the coupling of amines via an unexpected mechanism [96]. When phosphorus atoms were doped into graphene sheets, the P was more likely to

Table 2 Graphene-based materials in reduction catalytic reactions

Catalyst	Reaction system	Reaction conditions				Yield/%	Ref.
		Cat. dosage/mg	Capacity/mmol	Reductant/mL	Time/min		
rGO	Hydrogenation of nitrobenzene	10	4	2	240	94.2	[90]
NG	Reduction of 4-nitrophenol to 4-aminophenol	0.137	5×10^{-4}	2	21	100	[46]
NG	Reduction of 4-chloronitrobenzene	2	0.5	5	180	98	[91]
3D-NGF	Reduction of 4-nitrophenol to 4-aminophenol	0.15	2×10^{-4}	0.5	18	100	[86]
SG	Reduction of 4-nitrophenol to 4-aminophenol	1	0.02	2	60	100	[85]
3D SNC-GA-1000	Reduction of 4-nitrophenol to 4-aminophenol	3.572	0.002	3	7	100	[87]

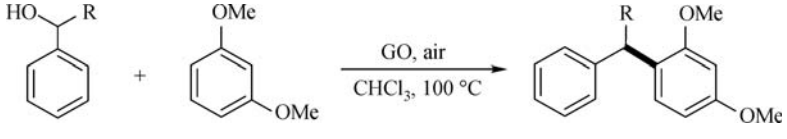

Scheme 4 GO-catalyzed Friedel-crafts alkylation of arenes with alcohols [92]

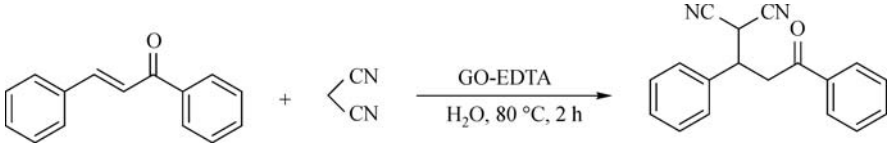

Scheme 5 Michael addition catalyzed by GO-DETA [94]

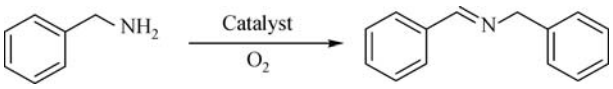

Scheme 6 Oxidation of benzylamine to N-benzylidene benzylamine [95]

be the catalytic site than the C because of its lower electronegativity (2.19 for P *versus* 2.55 for C). This is much different from N-doped graphene materials, whose active sites are the C atoms that are adjacent to the doping points since N (3.04) has a higher electronegativity than C (2.55). Table 3 summarizes the graphene-based materials that have been applied as metal-free catalysts in other organic catalytic reactions in recent years.

4 Summary and prospects

This review gives a brief overview of the fabrication methods for graphene-based catalysts and their catalytic performance for industrial oxidation, reduction and other important organic catalytic reactions. Graphene-based catalysts exhibit many advantages such as super-high specific surface areas, excellent heat and mass transfer performances, and good recoverabilities. However, there are still several challenges to the large-scale application of graphene-based catalysts in industry. So there is a need for continued research in this area. Three areas of particular need are: (1) although a variety of catalytic mechanisms have been proposed for metal-free catalytic systems, the mechanisms for these reactions still have not been adequately experimentally verified. Methods are needed to do this so because a proper understanding of the catalytic mechanisms will help guide the design of more efficient graphene-based catalysts. (2) The stability of current graphene-based catalysts is too poor to meet the high strength demands of industrial reactors. Although graphene materials can be used directly as catalysts, there is still a catalytic efficiency gap between metal-free catalysts and metal catalysts. Many researchers have tried to enhance the catalytic activity of graphene catalysts by heteroatom doping or functional modification, but the stability of these catalysts decreases as the number of defects in the intrinsic carbon material increases. This results in poor recycling and the need for large amounts of catalyst material. (3) Three-dimensional graphene-based metal-free catalysts have excellent heat and mass transfer performances and so these catalysts will continue to attract great attention. However, in order to meet the heat and mass transfer requirements of traditional industrial reactors, catalysts must have structural stability. Thus improving the physical strength of three-dimensional materials is an urgent problem that needs to be solved. Silicon carbide has often been used as a framework material because of its high strength, high rigidity, dimensional stability and excellent heat resistance [98]. Li et al. have fabricated silicon carbide-derived carbon nanocomposites and used them as a metal-free catalyst in the catalytic hydrochlorination of acetylene [99]. The acetylene conversion and vinyl chloride selectivity were 80% and 98%, respectively. This work demonstrated that a metal-free catalyst is a potential substitute for traditional mercury-based catalysts. However, the preparation process for this silicon carbide/carbon composite material is very complex. Better 3D structured metal-free catalysts with high stability and high catalytic performance still need to be developed.

In addition, the effective use of catalyst materials in traditional reaction equipment often creates problems resulting in sub-standard performances. A three-dimensional structured monolithic catalyst can effectively improve heat and mass transfer efficiency. However, the catalytic activities of many industrial catalysts do not achieve their theoretical mass transfer efficiencies when used in traditional reaction equipment, such as fix bed, trickle-bed, and batch reactors [100–102]. Recently, a rotating packed bed (RPB) reactor attracted much attention

Table 3 Graphene-based materials in other catalytic reactions

Catalyst	Reaction system	Reaction conditions				Level		Ref.
		Cat. dosage/mg	Capacity/mmol	Temp./K	Time/h	Conv./%	Select./%	
GO	Alkylation of arenes	0.3	0.144	373	15	98	100	[92]
GO	C-H arylation of benzene	0.3	0.4	393	2	100	87.6	[93]
BNHG	Aerobic oxidative coupling of amines	30	1	358	4	91	99	[95]
PG	Aerobic oxidative coupling of amines	4.3	0.4	373	12	100	82	[96]
Multi-functional graphene oxide	Cycloaddition reaction	100	28.6	393	3	89.5	99.7	[97]
Amine modification of graphene oxide	Michael addition	0.21	0.48	353	2	100	90	[94]

for its excellent performance in micromixing and mass transfer rates [103]. In the high-gravity field of a RPB reactor, the liquid was cut to liquid filaments, films, and droplets, which resulted in a large mass-transfer interfacial area and weak surface tension. Thus, this combination of a three-dimensional material and a RPB reactor shows promise for solving the mass transfer problem in both material and industrial aspects.

Looking forward to the future, the field of carbon based materials science is currently facing great challenges as well as unprecedented opportunities. We sincerely hope that this review can give some inspiration in the next few years for research that focus on the application of graphene-based catalysts in industrial catalytic reactions. From the perspective of development, the design of excellent performance graphene-based metal-free catalyst will take a fairly long time and require constant effort. But, one thing is certain that, with the development of multidisciplinary knowledge and the demand for green chemical industry, we have reason to believe that graphene-based materials will continue to open up widespread applications for the production of industrial chemicals and greatly replace traditional metal-based catalysts in the near future.

Acknowledgements We are grateful for financial support from the National Natural Science Foundation of China (Grant Nos. 21620102007 and 21622601), the Fundamental Research Funds for the Central Universities of China (No. BUCTRC201601), and the "111" project of China (No. B14004).

References

1. Chowdhury A D, Houben K, Whiting G T, Chung S H, Baldus M, Weckhuysen B M. Electrophilic aromatic substitution over zeolites generates Wheland-type reaction intermediates. Nature Catalysis, 2017, 1(1): 23–31
2. Hasany M, Malakootikhah M, Rahmanian V, Yaghmaei S. Effect of hydrogen combustion reaction on the dehydrogenation of ethane in a fixed-bed catalytic membrane reactor. Chinese Journal of Chemical Engineering, 2015, 23(8): 1316–1325
3. Koven A B, Tong S S, Farnood R R, Jia C Q. Alkali-thermal gasification and hydrogen generation potential of biomass. Frontiers of Chemical Science and Engineering, 2017, 11(3): 369–378
4. Tan C, Cao X, Wu X J, He Q, Yang J, Zhang X, Chen J, Zhao W, Han S, Nam G H, Sindoro M, Zhang H. Recent advances in ultrathin two-dimensional nanomaterials. Chemical Reviews, 2017, 117(9): 6225–6331
5. Georgakilas V, Perman J A, Tucek J, Zboril R. Broad family of carbon nanoallotropes: Classification, chemistry, and applications of fullerenes, carbon dots, nanotubes, graphene, nanodiamonds, and combined superstructures. Chemical Reviews, 2015, 115(11): 4744–4822
6. Ye M, Zhang Z, Zhao Y, Qu L. Graphene platforms for smart energy generation and storage. Joule, 2018, 2(2): 1–24
7. Wang D, Zhu L, Chen J F, Dai L. Can graphene quantum dots cause DNA damage in cells? Nanoscale, 2015, 7(21): 9894–9901
8. Tao H, Gao Y, Talreja N, Guo F, Texter J, Yan C, Sun Z. Two-dimensional nanosheets for electrocatalysis in energy generation and conversion. Journal of Materials Chemistry. A, Materials for Energy and Sustainability, 2017, 5(16): 7257–7284
9. Salehi E, Soroush F, Momeni M, Barati A, Khakpour A. Chitosan/polyethylene glycol impregnated activated carbons: Synthesis, characterization and adsorption performance. Frontiers of Chemical Science and Engineering, 2017, 11(4): 575–585
10. Xiang Z, Wang D, Xue Y, Dai L, Chen J F, Cao D. PAF-derived nitrogen-doped 3D carbon materials for efficient energy conversion and storage. Scientific Reports, 2015, 5(1): 8307–8314
11. Liu X, Dai L. Carbon-based metal-free catalysts. Nature Reviews Materials, 2016, 1(11): 16064–16075
12. Su D S, Wen G, Wu S, Peng F, Schlögl R. Carbocatalysis in liquid-phase reactions. Angewandte Chemie International Edition, 2017, 56(4): 936–964
13. Wang D, Wang Z, Zhan Q, Pu Y, Wang J X, Foster N R, Dai L. Facile and scalable preparation of fluorescent carbon dots for multifunctional applications. Engineering, 2017, 3(3): 402–408
14. Lv G, Wang H, Yang Y, Deng T, Chen C, Zhu Y, Hou X. Graphene oxide: A convenient metal-free carbocatalyst for facilitating aerobic oxidation of 5-hydroxymethylfurfural into 2,5-diformylfuran. ACS Catalysis, 2015, 5(8): 5636–5646
15. Wang S, Li Y, Fan X, Zhang F, Zhang G. β-Cyclodextrin functionalized graphene oxide: An efficient and recyclable adsorbent for the removal of dye pollutants. Frontiers of Chemical Science and Engineering, 2015, 9(1): 77–83
16. Liu Z, Wang W, Ju X, Xie R, Chu L. Graphene-based membranes for molecular and ionic separations in aqueous environments. Chinese Journal of Chemical Engineering, 2017, 25(11): 1598–1605
17. Kong X K, Chen C L, Chen Q W. Doped graphene for metal-free catalysis. Chemical Society Reviews, 2014, 43(8): 2841–2857
18. Deng D, Novoselov K S, Fu Q, Zheng N, Tian Z, Bao X. Catalysis with two-dimensional materials and their heterostructures. Nature Nanotechnology, 2016, 11(3): 218–230
19. Dai L, Xue Y, Qu L, Choi H J, Baek J B. Metal-free catalysts for oxygen reduction reaction. Chemical Reviews, 2015, 115(11): 4823–4892
20. Shinde S S, Lee C H, Sami A, Kim D H, Lee S U, Lee J H. Scalable 3-D carbon nitride sponge as an efficient metal-free bifunctional oxygen electrocatalyst for rechargeable Zn-Air batteries. ACS Nano, 2017, 11(1): 347–357
21. Huang P Y, Ruiz-Vargas C S, van der Zande A M, Whitney W S, Levendorf M P, Kevek J W, Garg S, Alden J S, Hustedt C J, Zhu Y, et al. Grains and grain boundaries in single-layer graphene atomic patchwork quilts. Nature, 2011, 469(7330): 389–392
22. Novoselov K S, Geim A K, Morozov S V, Jiang D, Zhang Y, Dubonos S V, Grigorieva I V, Firsov A A. Electric field effect in atomically thin carbon films. Science, 2004, 306(5696): 666–669
23. Tang P, Hu G, Li M, Ma D. Graphene-based metal-free catalysts for catalytic reactions in the liquid phase. ACS Catalysis, 2016, 6 (10): 6948–6958

24. Ma Y, Chen Y. Three-dimensional graphene networks: Synthesis, properties and applications. National Science Review, 2015, 2(1): 40–53
25. Senthilkumar K, Prabakar S R, Park C, Jeong S, Lah M S, Pyo M. Graphene oxide self-assembled with a cationic fullerene for high performance pseudo-capacitors. Journal of Materials Chemistry. A, Materials for Energy and Sustainability, 2016, 4(5): 1663–1670
26. Kim J, Sang W K, Yun H, Kim B J. Impact of size control of graphene oxide nanosheets for enhancing electrical and mechanical properties of carbon nanotube-polymer composites. RSC Advances, 2017, 7(48): 30221–30228
27. Ambrosetti A, Silvestrelli P L. Adsorption of rare-gas atoms and water on graphite and graphene by van der waals-corrected density functional theory. Journal of Physical Chemistry C, 2017, 115(9): 3695–3702
28. Esfandiyari T, Nasirizadeh N, Dehghani M, Ehrampoosh M H. Graphene oxide based carbon composite as adsorbent for Hg removal: Preparation, characterization, kinetics and isotherm studies. Chinese Journal of Chemical Engineering, 2017, 25(9): 1170–1175
29. Kato R, Minami S, Koga Y, Hasegawa M. High growth rate chemical vapor deposition of graphene under low pressure by RF plasma assistance. Carbon, 2016, 96: 1008–1013
30. Kim S, Song Y, Heller M J. Seamless aqueous arc discharge process for producing graphitic carbon nanostructures. Carbon, 2017, 120: 83–88
31. Patil I M, Lokanathan M, Kakade B. Three dimensional nanocomposite of reduced graphene oxide and hexagonal boron nitride as an efficient metal-free catalyst for oxygen electroreduction. Journal of Materials Chemistry. A, Materials for Energy and Sustainability, 2016, 4(12): 4506–4515
32. Tam T V, Kang S G, Babu K F, Oh E S, Leeb S G, Choi W M. Synthesis of B-doped graphene quantum dots as metal-free electrocatalyst for oxygen reduction reaction. Journal of Materials Chemistry. A, Materials for Energy and Sustainability, 2017, 5(21): 10537–10543
33. Lerf A, He H, Forster M, Klinowski J. Structure of graphite oxide revisited. Journal of Physical Chemistry B, 1998, 102(23): 4477–4482
34. Haag D R, Kung H H. Metal free graphene based catalysts: A review. Topics in Catalysis, 2014, 57(6-9): 762–773
35. Tu W, Zhou Y, Zou Z. Versatile graphene-promoting photocatalytic performance of semiconductors: Basic principles, synthesis, solar energy conversion, and environmental applications. Advanced Functional Materials, 2013, 23(40): 4996–5008
36. Shao P, Tian J, Yang F, Duan X, Gao S, Shi W, Luo X, Cui F, Luo S, Wang S. Identification and regulation of active sites on nanodiamonds: Establishing a highly efficient catalytic system for oxidation of organic contaminants. Advanced Functional Materials, 2018, 28(13): 1705295–1705302
37. Hummers W S Jr, Offeman R E. Preparation of graphitic oxide. Journal of the American Chemical Society, 1958, 80(6): 1339–1339
38. Chen J, Li Y, Huang L, Li C, Shi G. High-yield preparation of graphene oxide from small graphite flakes via an improved Hummers method with a simple purification process. Carbon, 2015, 81(1): 826–834
39. Bai J, Sun H, Yin X, Yin X, Wang S, Creamer A E, Xu L, Qin Z, He F, Gao B. Oxygen-content-controllable graphene oxide from electron-beam-irradiated graphite: Synthesis, characterization, and removal of aqueous lead. ACS Applied Materials & Interfaces, 2016, 8(38): 25289–25296 (Pb(II))
40. Gao Y J, Hu G, Zhong J, Shi Z J, Zhu Y S, Su D S, Wang J G, Bao X H, Ma D. Nitrogen-doped sp^2-hybridized carbon as a superior catalyst for selective oxidation. Angewandte Chemie International Edition, 2013, 52(7): 2109–2113
41. Kumar R, Singh R K, Vaz A R, Savu R, Moshkalev S A. Self-assembled and one-step synthesis of interconnected 3D network of Fe_3O_4/reduced graphene oxide nanosheets hybrid for high performance supercapacitor electrode. ACS Applied Materials & Interfaces, 2017, 9(10): 8880–8890
42. Hu G, Xu C, Sun Z, Wang S, Cheng H M, Li F, Ren W. 3D graphene-foam-reduced-graphene-oxide hybrid nested hierarchical networks for high-performance Li-S batteries. Advanced Materials, 2016, 28(8): 1603–1609
43. Mu X, Yuan B, Feng X, Qiu S, Song L, Hu Y. The effect of doped heteroatoms (nitrogen, boron, phosphorus) on inhibition thermal oxidation of reduced graphene oxide. RSC Advances, 2016, 6 (107): 105021–105029
44. Aunkor M H, Mahbubul I M, Saidurb R, Metselaar H C. The green reduction of graphene oxide. RSC Advances, 2016, 6(33): 27807–27828
45. Sykam N, Rao G M. Room temperature synthesis of reduced graphene oxide nanosheets as anode material for supercapacitors. Materials Letters, 2014, 204: 169–172
46. Kong X K, Sun Z, Chen M, Chen C, Chen Q W. Metal-free catalytic reduction of 4-nitrophenol to 4-aminophenol by N-doped graphene. Energy & Environmental Science, 2013, 6(11): 3260–3266
47. Xu K, Fu Y, Zhou Y, Hennersdorf F, Machata P, Vincon I, Weigand J J, Popov A A, Berger R, Feng X. Cationic nitrogen-doped helical nanographenes. Angewandte Chemie International Edition, 2017, 56(50): 15876–15881
48. Tao H, Yan C, Robertson A W, Gao Y, Ding J, Zhang Y, Maa T, Sun Z. N-doping of graphene oxide at low temperature for the oxygen reduction reaction. Chemical Communications, 2017, 53 (5): 873–876
49. Wang X, Sun G, Routh P, Kim D H, Huang W, Chen P. Heteroatom-doped graphene materials: Syntheses, properties and applications. Chemical Society Reviews, 2014, 43(20): 7067–7098
50. Wei D, Liu Y, Wang Y, Zhang H, Huang L, Yu G. Synthesis of N-doped graphene by chemical vapor deposition and its electrical properties. Nano Letters, 2009, 9(5): 1752–1758
51. Vineesh T V, Kumar M P, Takahashi C, Kalita G, Alwarappan S, Pattanayak D K, Narayanan T N. Bifunctional electrocatalytic activity of boron-doped graphene derived from boron carbide. Advanced Energy Materials, 2015, 5(17): 1500658–1500665
52. Putri L K, Ng B J, Ong W J, Lee H W, Chang W S, Chai S P. Heteroatom nitrogen- and boron-doping as a facile strategy to improve photocatalytic activity of standalone reduced graphene oxide in hydrogen evolution. ACS Applied Materials & Interfaces, 2017, 9(5): 4558–4569

53. Fang Y, Wang X. Metal-free boron-containing heterogeneous catalysts. Angewandte Chemie International Edition, 2017, 56(49): 15506–15518
54. Yu C, Liu Z, Meng X, Lu B, Cui D, Qiu J. Nitrogen and phosphorus dual-doped graphene as a metal-free high-efficiency electrocatalyst for triiodide reduction. Nanoscale, 2016, 8(40): 17458–17464
55. Xu J, Shui J, Wang J, Wang M, Liu H K, Dou S X, Jeon I Y, Seo J M, Baek J B, Dai L. Sulfur graphene nanostructured cathodes via ball-milling for highperformance lithium sulfur batteries. ACS Nano, 2014, 8(10): 10920–10930
56. Xu J, Jeon I Y, Seo J M, Dou S, Dai L, Baek J B. Edge-selectively halogenated graphene nanoplatelets (XGnPs, X = Cl, Br, or I) prepared by ball-milling and used as anode materials for lithium-ion batteries. Advanced Materials, 2014, 26(43): 7317–7323
57. Xu J, Ma J, Fan Q, Guo S, Dou S. Recent progress in the design of advanced cathode materials and battery models for high-performance lithium-X (X = O_2, S, Se, Te, I_2, Br_2) batteries. Advanced Materials, 2017, 29(28): 1606454–1606473
58. Xiang Z, Cao D, Huang L, Shui J, Wang M, Dai L. Nitrogen-doped holey graphitic carbon from 2D covalent organic polymers for oxygen reduction. Advanced Materials, 2014, 26(2): 3315–3320
59. Zhang J, Dai L. Nitrogen, phosphorus, and fluorine tri-doped graphene as a multifunctional catalyst for self-powered electrochemical water splitting. Angewandte Chemie International Edition, 2016, 55(42): 13296–13300
60. Du R, Zhao Q, Zhang N, Zhang J. Macroscopic carbon nanotube-based 3D monoliths. Small, 2015, 11(27): 3263–3289
61. Worsley M A, Charnvanichborikarn S, Montalvo E, Shin S J, Tylski E D, Lewicki J P, Nelson A J, Satcher J H Jr, Biener J, Baumann T F, et al. Toward macroscale, isotropic carbons with graphene-sheet-like electrical and mechanical properties. Advanced Functional Materials, 2014, 24(27): 4259–4264
62. Charon E, Rouzaud J N, Aléon J. Graphitization at low temperatures (600–1200 °C) in the presence of iron implications in planetology. Carbon, 2014, 66: 178–190
63. Xia J, Zhang N, Chong S, Li D, Chen Y, Sun C. Three-dimensional porous graphene-like sheets synthesized from biocarbon via low-temperature graphitization for a supercapacitor. Green Chemistry, 2018, 20(3): 694–700
64. Wang H, Li X B, Gao L, Wu H L, Yang J, Cai L, Ma T B, Tung C H, Wu L Z, Yu G. Three-dimensional graphene networks with abundant sharp edge sites for efficient electrocatalytic hydrogen evolution. Angewandte Chemie International Edition, 2018, 57(1): 192–197
65. Ren H, Tang M, Guan B, Wang K, Yang J, Wang F, Wang M, Shan J, Chen Z, Wei D, et al. Hierarchical graphene foam for effcient omnidirectional solar-thermal energy conversion. Advanced Materials, 2017, 29(38): 1702590–1702596
66. Shao Y, El-Kady M F, Lin C W, Zhu G, Marsh K L, Hwang J Y, Zhang Q, Li Y, Wang H, Kaner R B. 3D freeze-casting of cellular graphene films for ultrahigh-power-density supercapacitors. Advanced Materials, 2016, 28(31): 6719–6726
67. Compton B G, Lewis J A. 3D-printing of lightweight cellular composites. Advanced Materials, 2014, 26(34): 5930–5935
68. Zhu C, Han T Y, Duoss E B, Golobic A M, Kuntz J D, Spadaccini C M, Worsley M A. Highly compressible 3D periodic graphene aerogel microlattices. Nature Communications, 2015, 6(1): 6962–6969
69. Sha J, Li Y, Salvatierra R V, Wang T, Dong P, Ji Y, Lee S K, Zhang C, Zhang J, Smith R H, et al. Three-dimensional printed graphene foams. ACS Nano, 2017, 11(7): 6860–6867
70. Qi W, Yan P, Su D S. Oxidative dehydrogenation on nanocarbon: Insights into the reaction mechanism and kinetics via *in situ* experimental methods. Accounts of Chemical Research, 2018, 51 (3): 640–648
71. Guo X, Qi W, Liu W, Yan P, Li F, Liang C, Su D S. Oxidative dehydrogenation on nanocarbon: Revealing the catalytic mechanism using model catalysts. ACS Catalysis, 2017, 7(2): 1424–1427
72. Liu W, Chen B, Duan X, Wu K H, Qi W, Guo X, Zhang B, Su D S. Molybdenum carbide modified nanocarbon catalysts for alkane dehydrogenation reactions. ACS Catalysis, 2017, 7(9): 5820–5827
73. Yang X, Cao Y, Yu H, Huang H, Wang H, Peng F. Unravelling the radical transition during the carbon-catalyzed oxidation of cyclohexane by *in situ* electron paramagnetic resonance in the liquid phase. Catalysis Science & Technology, 2017, 7(9): 4431–4443
74. Yang J H, Sun G, Gao Y, Zhao H, Tang P, Tan J, Lu A H, Ma D. Direct catalytic oxidation of benzene to phenol over metal-free graphene-based catalyst. Energy & Environmental Science, 2013, 6(3): 793–798
75. Indrawirawan S, Sun H, Duan X, Wang S. Low temperature combustion synthesis of nitrogen-doped graphene for metal-free catalytic oxidation. Journal of Materials Chemistry. A, Materials for Energy and Sustainability, 2015, 3(7): 3432–3440
76. Duan X, O'Donnell K, Sun H, Wang Y, Wang S. Sulfur and nitrogen co-doped graphene for metal-free catalytic oxidation reactions. Small, 2015, 11(25): 3036–3044
77. Huang Z F, Bao H W, Yao Y Y, Lu W Y, Chen W X. Novel green activation processes and mechanism of peroxymonosulfate based on supported cobalt phthalocyanine catalyst. Applied Catalysis B: Environmental, 2014, 154: 36–43
78. Diao J, Liu H, Wang J, Feng Z, Chen T, Miao C, Yang W, Su D S. Porous graphene-based material as an efficient metal free catalyst for the oxidative dehydrogenation of ethylbenzene to styrene. Chemical Communications, 2015, 51(16): 3423–3425
79. Dhakshinamoorthy A, Latorre-Sanchez M, Asiri A M, Primo A, Garcia H. Sulphur-doped graphene as metal-free carbocatalysts for the solventless aerobic oxidation of styrenes. Catalysis Communications, 2015, 65: 10–13
80. Gonçalves G B, Pires S G, Simoes M Q, Nevesb M S, Marques P P. Three-dimensional graphene oxide: A promising green and sustainable catalyst for oxidation reactions at room temperature. Chemical Communications, 2014, 50(57): 7673–7676
81. Long J, Xie X, Xu J, Gu Q, Chen L, Wang X. Nitrogen-doped graphene nanosheets as metal-free catalysts for aerobic selective oxidation of benzylic alcohols. ACS Catalysis, 2012, 2(4): 622–631
82. Rizescu C, Podolean I, Albero J, Parvulescu V I, Coman S M, Bucur C, Puchec M. Garcia H. N-Doped graphene as a metal-free catalyst for glucose oxidation to succinic acid. Green Chemistry, 2017, 19(8): 1999–2005

83. Gu Q, Wen G, Ding Y, Wu K H, Chen C, Su D. Reduced graphene oxide: A metal-free catalyst for aerobic oxidative desulfurization. Green Chemistry, 2017, 19(4): 1175–1181
84. Gu S, Wunder S, Lu Y, Ballauff M, Fenger R, Rademann K, Jaquet B, Zaccone A. Kinetic analysis of the catalytic reduction of 4 nitrophenol by metallic nanoparticles. Journal of Physical Chemistry C, 2014, 118(32): 18618–18625
85. Wang Z, Su R, Wang D, Shi J, Wang J X, Pu Y, Chen J F. Sulfurized graphene as efficient metal-free catalysts for reduction of 4-nitrophenol to 4-aminophenol. Industrial & Engineering Chemistry Research, 2017, 56(46): 13610–13617
86. Liu J, Yan X, Wang L, Kong L, Jian P. Three-dimensional nitrogen-doped graphene foam as metal-free catalyst for the hydrogenation reduction of p-nitrophenol. Journal of Colloid and Interface Science, 2017, 497: 102–107
87. Pan J, Song S, Li J, Wang F, Ge X, Yao S, Wang X, Zhang H. Solid ion transition route to 3D S-N-codoped hollow carbon nanosphere/graphene aerogel as a metal-free handheld nanocatalyst for organic reactions. Nano Research, 2017, 10(10): 3486–3495
88. Qiu B, Xing M, Zhang J. Recent advances in three-dimensional graphene based materials for catalysis applications. Chemical Society Reviews, 2018, 47(6): 2165–2216
89. Wang Z, Pu Y, Wang D, Shi J, Wang J X, Chen J F. 3D-foam-structured nitrogen-doped graphene-Ni catalyst for highly efficient nitrobenzene reduction. AIChE Journal. American Institute of Chemical Engineers, 2018, 64(4): 1330–1338
90. Gao Y, Ma D, Wang C, Guan J, Bao X. Reduced graphene oxide as a catalyst for hydrogenation of nitrobenzene at room temperature. Chemical Communications, 2011, 47(8): 2432–2434
91. Yang F, Chi C, Wang C, Wang Y, Li Y. High graphite N content in nitrogen-doped graphene as an efficient metal-free catalyst for reduction of nitroarenes in water. Green Chemistry, 2016, 18(15): 4254–4262
92. Hu F, Patel M, Luo F, Flach C, Mendelsohn R, Garfunkel E, He H, Szostak M. Graphene-catalyzed direct friedel-crafts alkylation reactions: mechanism, selectivity, and synthetic utility. Journal of the American Chemical Society, 2015, 137(45): 14473–14480
93. Gao Y, Tang P, Zhou H, Zhang W, Yang H, Yan N, Hu G, Mei D, Wang J, Ma D. Graphene oxide catalyzed C–H bond activation: The importance of oxygen functional groups for biaryl construction. Angewandte Chemie, 2016, 128(9): 3176–3180
94. Yang A, Li J, Zhang C, Zhang W, Ma N. One-step amine modification of graphene oxide to get a green trifunctional metal-free catalyst. Applied Surface Science, 2015, 346: 443–450
95. Li X H, Antonietti M. Polycondensation of boron- and nitrogen-codoped holey graphene monoliths from molecules: Carbocatalysts for selective oxidation. Angewandte Chemie, 2013, 52(17): 4670–4674
96. Yang F, Fan X, Wang C, Yang W, Hou L, Xu X, Feng A, Dong S, Chen K, Wang Y, et al. P-doped nanomesh graphene with high-surface-area as an efficient metal-free catalyst for aerobic oxidative coupling of amines. Carbon, 2017, 121: 443–451
97. Lan D H, Chen L, Au C T, Yin S F. One-pot synthesized multi-functional graphene oxide as a water-tolerant and efficient metal-free heterogeneous catalyst for cycloaddition reaction. Carbon, 2015, 93: 22–31
98. Lacroix M, Dreibine L, Tymowski B, Vigneron F, Edouard D, Bégin D, Nguyen P, Pham C, Savin-Poncet S, Luck F, Ledoux M J, Pham-Huu C. Silicon carbide foam composite containing cobalt as a highly selective and re-usable Fischer-ropsch synthesis catalyst. Applied Catalysis A, General, 2011, 397(1): 62–72
99. Li X, Pan X, Yu L, Ren P, Wu X, Sun L, Jiao F, Bao X. Silicon carbide-derived carbon nanocomposite as a substitute for mercury in the catalytic hydrochlorination of acetylene. Nature Communications, 2014, 5(1): 3688–3694
100. Haase S, Weiss M, Langsch R, Bauer T, Lange R. Hydrodynamics and mass transfer in three-phase composite minichannel fixed-bed reactors. Chemical Engineering Science, 2013, 94(5): 224–236
101. Leung P C, Recasens F, Smith J M. Hydration of isobutene in a trickle-bed reactor: Wetting efficiency and mass transfer. AIChE Journal. American Institute of Chemical Engineers, 1987, 33(6): 996–1007
102. Leveneur S, Wärnå J, Salmi T, Murzin D Y, Estel L. Interaction of intrinsic kinetics and internal mass transfer in porous ion-exchange catalysts: Green synthesis of peroxycarboxylic acids. Chemical Engineering Science, 2009, 64(19): 4101–4114
103. Chu G W, Song Y J, Zhang W J, Luo Y, Zou H K, Xiang Y, Chen J F. Micromixing efficiency enhancement in a rotating packed bed reactor with surface-modified nickel foam packing. Industrial & Engineering Chemistry Research, 2015, 54(5): 1697–1702